

## Structural and optical analysis of SnO<sub>2</sub> thin films BY Spray Pyrolysis

S. Roguai<sup>1,\*</sup>, A. Djelloul

<sup>1</sup>LASPI2A: Laboratory Properties and interatomic Interactions, University Abbes Laghrour, Khenchela 40000, Algeria.

\*Corresponding author: rog.sabrina@yahoo.fr ; Tel.: +213 00 00 00 ; Fax: +21300 00 00

### ARTICLE INFO

#### Article History:

Received : 02/02/2020  
Accepted : 29/09/2020

#### Key Words:

Thin films;  
X-ray diffraction; FTIR spectroscopy;  
Optical properties;  
Photoluminescence spectroscopy.

### ABSTRACT/RESUME

**Abstract:** SnO<sub>2</sub> thin films were deposited by ultrasound pyrolysis spray technique at 450°C. The films were characterized by X-ray diffraction, Fourier transformed infrared (FTIR), ultraviolet–visible and Photoluminescence spectroscopy. The tetragonal rutile-type structure was confirmed by X-ray diffraction with an average crystallite size of 35 nm. In addition, the FTIR study indicated the existence of two distinct characteristic absorptions which correspond to (O-Sn-O) deformations and (O-Sn) stretching modes. For the optical properties, the band gap energy was determined by Wemple-DiDomenico model. PL properties are ascribed to the presence of intrinsic defects.

### I. Introduction

Oxides (TCO) are interesting materials because of their unique characteristics such as high electrical conductivity and high transparency which makes ideal candidates for many applications such as optoelectronics, photovoltaic and catalytic applications [1] Zinc Oxide (ZnO) & Tin Dioxide (SnO<sub>2</sub>) are among the TCOs which offer most accurately an exceptional choice for the electronic devices synthesis on the hand [2-4]. And they are used to obtain thin films for the purpose of manufacturing solar cells, on the other hand [1]

SnO<sub>2</sub> is n-type semiconductor with high conductivity due to the presence of structural defects (VO) in its rutile tetragonal structure. In addition to their transparency with a gap energy of 3.6 eV at 300K [5-7] Several techniques have been used to develop tin oxide thin layers of such as sol-gel [8], pulsed laser deposition [9], RF sputtering [10] and spray pyrolysis [11-16]. The ultrasonic pyrolysis spray has many advantages, such as their simplicity to prepare thin films with large surface area from high purity materials. The obtained films have a great homogeneity, a well controlled stoichiometry, can be treated at low temperature. The best advantage is its low cost [17].

In this work, we studied the structural and optical properties, of SnO<sub>2</sub> thin films deposited by the ultrasound pyrolysis spray technique (USP). Theoretical relationships are used to obtain the dispersion parameters of the films from a single experimental transmission spectrum.

### II. Experimental Part

#### II.1. Film preparation

SnO<sub>2</sub> thin films were prepared by USP method. The utilized solution for the elaborated films has the following composition: 0.01 M of tin chloride [SnCl<sub>4</sub>, 2H<sub>2</sub>O] (Fulka 99.9 %) is used as the Sn source; 50 ml deionized water (resistivity=18.2 MΩ.cm); 20 ml CH<sub>3</sub>OH (Merck 99.5 %); 30 ml C<sub>2</sub>H<sub>5</sub>OH (Merck 99.5 %). Details are listed in the works [17]

#### II.2. Characterization techniques

The thin films were characterized by XRD, SEM, FTIR and optical absorption and photoluminescence properties are thoroughly studied. Structural properties recorded using diffractometer high resolution Rigaku Ultima IV powder equipped with Cu-Kα radiation (λ= 1.5418 Å). The surface morphologies of nanoparticles were

characterized by using scanning electron microscopy (SEM) (FEI Quanta TM 250 FEG). The optical properties were estimated utilizing a Perkin Elmer UV-VIS-NIR Lambda 19 spectrophotometer in the 190-1800 nm spectral range. The FTIR spectra were recorded using Thermo-Nicolet equipment in the 4000-400  $\text{cm}^{-1}$  region. Photoluminescence measurements of prepared samples were examined using Perkin-Elmer LS 45 Fluorescence spectrometer with excitation wavelength of 350 nm.

### III. Results and discussion

#### III.1. Structure analysis

X-ray diffraction patterns of as-prepared pure  $\text{SnO}_2$  in Figure 1 reveal the formation of tetragonal Rutile structure as confirmed with (JCPDS Card No. 00-041-1445) with space group  $P4_2/mnm$ . located at  $2\theta$  values  $27.2^\circ$ ,  $34.4^\circ$ ,  $38.4^\circ$ ,  $52.2^\circ$ ,  $55.1^\circ$  and  $62.1^\circ$  and their Miller indices were (110), (101), (200), (211), (220) and (310) respectively [18,19]. A preferred orientation along (110) direction [20] is observed, no apparent reflection (impurities) were observed which indicated the synthesized samples were purely single phase [21]

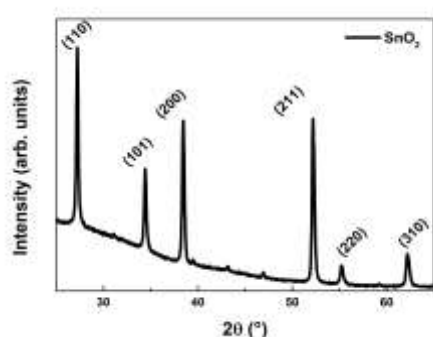


Figure 1. XRD patterns of  $\text{SnO}_2$ .

The lattice parameters and crystallite size calculated from Scherrer's formula [22]:

$$D = \frac{0.9\lambda}{\beta \cos\theta} \quad (1)$$

where 0.94 is a shape factor,  $\lambda$  represents the X-ray wavelength of the radiation source used for the measurement ( $\lambda_{\text{Cu}}=0.154$  nm),  $\beta$  (rad) is the line width full width half maximum, and  $\theta$  is the Bragg's angle (Equation. 2).

$$2d_{hkl} \sin(\theta) = n\lambda \quad (2)$$

Where,

$h$ ,  $k$ , and  $l$  integers,  $d$  is spacing between the planes in the atomic lattice. Using standard equations [23], the lattice parameters 'a' and 'c', dislocation density and unit cell volume of tetragonal structure of  $\text{SnO}_2$  nanoparticles were determined from the diffraction peaks of (110) and (101) were, respectively, calculated from the following equations:

$$\frac{1}{d} = \left[ \frac{h^2 + k^2 + l^2}{a^2} \right] + \frac{l^2}{c^2} \quad (3)$$

$$\delta = \frac{1}{d^2} \quad (4)$$

$$V = a^2c. \quad (5)$$

where,  $\delta$  Dislocation density,  $V$  unit cell volume From Table 1, it was observed that the lattice parameters and cell volume of  $\text{SnO}_2$  nanoparticles were decreased compared to that of pure tin oxide nanoparticles. which in agreement with [24].

Table 1. Structural parameters of  $\text{SnO}_2$  nanoparticles

	$2\theta$ value ( $^\circ$ )	FWHM ( $\beta$ ) ( $^\circ$ )	d-Value ( $\text{A}^\circ$ )	a=b ( $\text{A}^\circ$ )	c ( $\text{A}^\circ$ )	c/a	V ( $\text{A}^3$ )	Average crystal size (D) (nm)	Micro-strain (%)
<b>SnO<sub>2</sub></b>	27.2422	0.2466	3.3470	4.7333	3.1854	0.6729	71.3661	33	3.03

#### III.2. Morphological studies of $\text{SnO}_2$ nanoparticles

Figure 2 shows nano-particles of SEM images of  $\text{SnO}_2$ . The surface morphology is uniform and

appears as a distribution of small granular shaped particles evenly distributed throughout it [25]. Crystalline size: 100 nm.

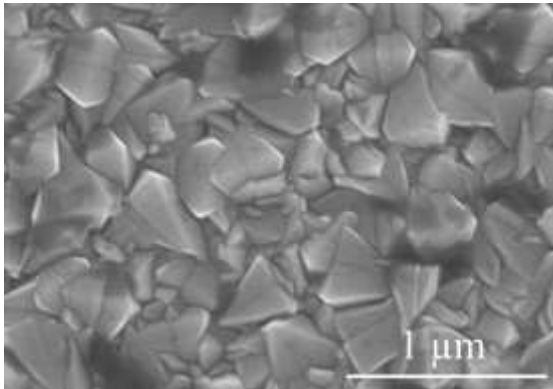


Figure 2. SEM images of SnO<sub>2</sub> thin films

### III.3. FTIR Analysis

FT-IR spectroscopy is used to identify the adsorbed functional group from their frequencies. Figures 3, 4 shows the FTIR spectra for SnO<sub>2</sub> film recorded between 400cm<sup>-1</sup> and 4000cm<sup>-1</sup> at room temperature. two large peaks around 3444cm<sup>-1</sup> and 1624cm<sup>-1</sup> are observed due to the vibrations of the hydrogen bond involved in the O-H oscillators in the adsorbed water molecules and in the alcohol respectively [26] and small peaks around 1023cm<sup>-1</sup>, 1384 cm<sup>-1</sup>and 2356 cm<sup>-1</sup>denote the hydrogen bonds involved in O-H oscillators and peaks around 2849 cm<sup>-1</sup> and 2356 cm<sup>-1</sup>may be due to the CO<sub>2</sub> absorption from the ambient air atmosphere [27-29]. And two bands appearing around 574 cm<sup>-1</sup>and 665 cm<sup>-1</sup>for are due to the Sn-O-Sn vibration and the Sn-O bond in SnO<sub>2</sub> which confirms the existence of SnO<sub>2</sub> [26, 30-32].

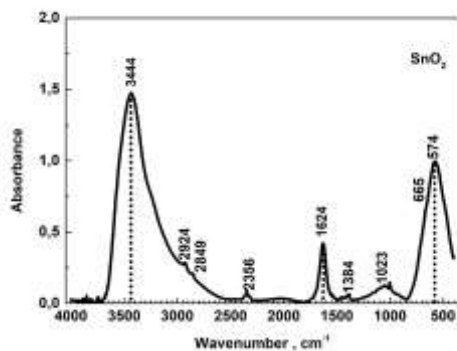


Figure 3. FTIR spectra of SnO<sub>2</sub> films grown onto glass substrate by ultrasonic spray pyrolysis at 450°C in the game 400-4000 cm<sup>-1</sup>

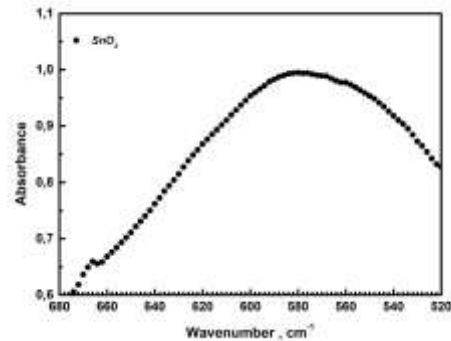


Figure 4. FTIR spectra of SnO<sub>2</sub> films grown onto glass substrate by ultrasonic spray pyrolysis at 450°C in the interval 520-680 cm<sup>-1</sup>.

### III.4. Optical properties

Figure 5 shows the transmission spectrum of SnO<sub>2</sub> deposited on a glass substrate. the spectrum obtained as a function of the wavelength (190-1100 nm), The solid curve corresponds to the curve fitting and the symbol represents the experimental data. The Figures reveal a reasonably good fitting to the experimental data [33]. although the general pattern of the spectra is that they are composed of two regions:

- A region of strong absorption. This region corresponds to the fundamental absorption ( $\lambda < 400$  nm) in the films. This absorption is due to the interband electronic transition. The variation of the transmission in this region is exploited for the determination of the gap.
- A region of high transparency located between 400 and 1100nm, the values of the transmission is of the order of 68.9%. this value gives our thin layers obtained by pyrolysis Spray, the transparency character in the visible.

The value obtained from the E<sub>g</sub> as well as the thickness and *n* at 598 nm, extracted by fitting [33] the experimental data are listed in Table 2. The value of the bandgap obtained is in accordance with the known value of SnO<sub>2</sub> [34, 35].

**Table 2.** Dispersion parameters of the films extracted by fitting the experimental data [33].

	Thickness (nm)	$E_g$ (eV)	$n$ at 598 (nm)
SnO <sub>2</sub>	583	3.838	1.697

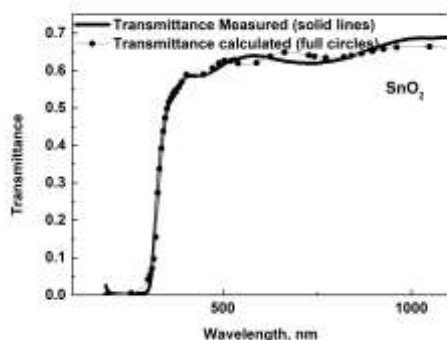


**Figure 5.** Transmission spectrum of SnO<sub>2</sub> films deposited on glass substrate at 450 °C. Measured (full circles) and calculated (solid lines) transmittance spectra of films.

Figure 6 present calculated refractive indices [33] of SnO<sub>2</sub> film. It is observed that the value is equal to 1.697.

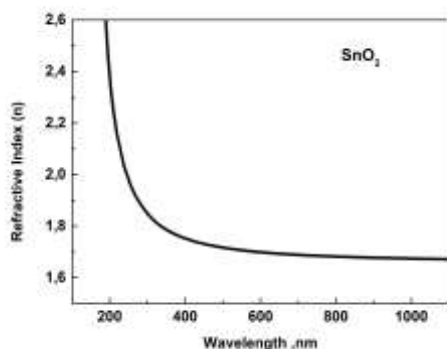


**Figure 6.** Refractive index of SnO<sub>2</sub> films grown on glass substrate at  $T_s = 450$  °C

### III.5. Photoluminescence properties

In Figure 7, PL spectra consist of four emission peaks centered about 407, 419, 484 and 529 nm. As energy corresponding to all the observed emission peaks (3.04, 2.95, 2.56 and 2.34 eV) is lower than the band gap energy of the film [17,34]. The first two bands P1 and P2 located in the violet emission show the donor-acceptor recombination (DAP) due to the electronic transition between the two valence and conduction band is exactly donor close to the (BC) and acceptor levels near the top of the (BV)

[17,35]. The two emissions P3 and P4 may be due to the electronic transition from the deep donor level formed by the oxygen vacancies to the valence band in the film [17,36].

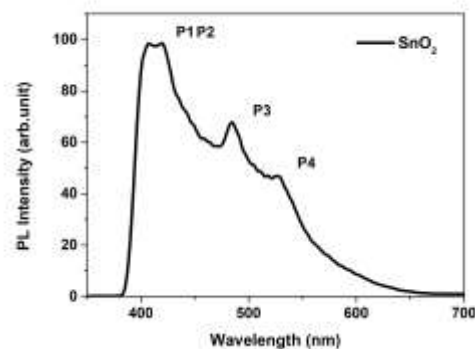


**Figure 7.** PL spectra of SnO<sub>2</sub> thin films measured at room temperature.

## IV. Conclusion

SnO<sub>2</sub> Thin layers were deposited by the Pyrolysis Spray technique on glass substrates at 450 °C at 30 min.

The obtained films are polycrystalline with the tetragonal structure and have a (110) preferred orientation, found uniform surface morphology with small granular shaped particles distributed throughout the surface. The FTIR study indicated the existence of two distinct characteristic absorption peaks at 574cm<sup>-1</sup> and 665 cm<sup>-1</sup> for the mode of vibration of deformations (O-Sn-O) and of stretching (O-Sn) respectively. From the transmittance spectra, we have deduced the optical gap  $E_g$  as well as the thickness and the refractive index of SnO<sub>2</sub> films by the model of Wemple and DiDomenico. Photoluminescence spectroscopy reveals the presence of intrinsic defects.

## Acknowledgments

The authors would like to thank the National Project Research (PNR) and LASPI<sup>2</sup>A Laboratory of Khenchela University (Algeria) for their financial support of this research project.

## V. References

1. Lekshmy, S.S.; Daniel, G.P.; Joy, K. Microstructure and physical properties of sol gel derived SnO<sub>2</sub>: Sb thin films for optoelectronic applications. *Applied Surface Science* 274 (2013) 95-100
2. Tharsika, T.; Haseeb, A.S.M.A.; Sabri, M.F.M. Structural and optical properties of ZnO-SnO<sub>2</sub> mixed thin films deposited by spray pyrolysis. *Thin Solid Films* 558 (2014) 283-288.

3. Paliwal, A.; Sharma, A.; Tomar, M.; Gupta, V. Carbon monoxide (CO) optical gas sensor based on ZnO thin films. *Sensors and Actuators, B: Chemical* 250 (2017) 679-685.
4. Al-Jawad, S.M.H. Influence of multilayer deposition on characteristics of nanocrystalline SnO<sub>2</sub> thin films produce by sol-gel technique for gas sensor application. *Optik (Stuttg)* 146 (2017) 17-26.
5. Sinha, A.K.; Manna, P.K.; Pradhan, M.; Mondal, C.; Yusuf, S.M.; Pal, T. Tin oxide with a p- n heterojunction ensures both UV and visiblelight photocatalytic activity. *Royal Society of Chemistry Adv* 4 (2014) 208-211.
6. Kamble, V.B.; Umarji, A.M. Defect induced optical bandgap narrowing in undoped SnO<sub>2</sub> nanocrystals. *AIP Advances* 3 (2013) 082120-082125.
7. Ginley, D.S.; Bright, C. Transparent conducting oxides. *MRS Bulletin* 25 (2000) 15-18.
8. Soitah, T.N.; Chunhui, Y.; Liang, S. Structural, optical and electrical properties of Fe-doped SnO<sub>2</sub> fabricated by sol-gel dip coating technique. *Materials Science in Semiconductor Processing* 13 (2010) 125- 131.
9. Gaidi, M.; Hajjaji, A.; Smirani, R.; Bessais, B.; El Khakani, M.A. Structure and photoluminescence of ultrathin films of SnO<sub>2</sub> nanoparticles synthesized by means of pulsed laser deposition. *Journal of Applied Physics* 108 (2010) 1-5.
10. Korber, C.; Agoston, P.; Klein, A. Surface and bulk properties of sputter Deposited undoped and Sb-doped SnO<sub>2</sub> thin films. *Sensors Actuators B* 139 (2009) 665-672.
11. Acosta, D.R.; Estrada, W.; Castanedo, R.; Maldonado, A.; Valunzuela, MA. Structural and surface studies of tin oxide films doped with fluorine. *Thin Solid Films* 375 (1998) 147-150.
12. Korotcenkov, G.; DiBattista, M.; Schwank, J.; Brinzari, V. Structural characterization of SnO<sub>2</sub> gas sensing films deposited by spray pyrolysis. *Materials Science and Engineering: B* 77 (2000) 33-39.
13. Lopes, A.; Fortunato, E.; Nunes, P.; Vilarinho, P.; Martins, R. Correlation between the microscopic and macroscopic characteristics of SnO<sub>2</sub> thin film gas sensors. *International Journal of Inorganic Materials* 3 (2001) 1349-1351.
14. Elangovan, E.; Singh, M.P.; Ramamurthi, K. Studies on structural and electrical properties of spray deposited SnO<sub>2</sub>:F thin films as a function of film thickness. *Materials Science and Engineering: B* 113 (2004) 143-148.
15. Ait Aouaj, M.; Diaz, R.; Belayachi, A.; Rueda, F.; Abd-Lefdil, M. Comparative study of ITO and FTO thin films grown by spray pyrolysis. *Materials Research Bulletin* 44 (2009) 1458-1461
16. Kamoun Allouche, N.; Ben Nasr, T.; Kamoun Turki, N.; Castagné, M. Characterization of heterojunctions based on airless spray deposited CuInS<sub>2</sub> thin films on different underlayers. *Energy Procedia* 2 (2010) 91-101.
17. Roguai, S.; Djelloul, A. Synthesis and evaluation of the structural, microstructural, optical and magnetic properties of Zn<sub>1-x</sub>Co<sub>x</sub>O thin films grown onto glass substrate by ultrasonic spray pyrolysis. *Journal of Applied Physics A* (2019) 125:816 doi.org/10.1007/s00339-019-3118-3
18. Khan Zulfiqar, R.; Zaman, Y. Effect of annealing on structural, dielectric, transport and magnetic properties of (Zn, Co) co-doped SnO<sub>2</sub> nanoparticles. *Journal of Materials Science: Materials in Electronics* 27 (2016) 4003-4010.
19. Khan Zulfiqar, R.; Fashu, S.; Zaman, Y. Magnetic and dielectric properties of (Co, Zn) codoped SnO<sub>2</sub> diluted magnetic semiconducting nanoparticles. *Journal of Materials Science: Materials in Electronics* 27 (2016) 5960-5966.
20. Pascariu Dorneanu, P.; Airinei, A.; Grigoras, Mircea.; Fifere, N.; Sacarescu, L.; Lupu, N.; Stoleriu, L. Structural, optical and magnetic properties of Ni doped SnO<sub>2</sub> nanoparticles. *Journal of Alloys and Compounds* 668 (2016) 65-72.
21. Cullity, B.D. *Elements of X-Ray Diffraction*. Addison-Wesley, Reading.; MA (1978) pp. 44-45.
22. Ayeshamariam, A.; Sanjeeviraja, C.; PerumalSamy, R. Synthesis, structural and optical characterizations of SnO<sub>2</sub> nanoparticles. *Journal of Photonics and Spintronics* 2 (2013) 2324-8572.
23. Bannur, M.S.; Albin Antony, K.I.; Maddani, P.; Poornesh, P.; Ashok Rao, Choudhari, K.S. Tailoring the nonlinear optical susceptibility  $\chi^{(3)}$ , photoluminescence and optical band gap of nanostructured SnO<sub>2</sub> thin films by Zn doping for photonic device applications. *Physica: E* (2018) DOI: 10.1016/j.physe.2018.06.025
24. Eqbal, E.; Raphael, R.; Saji, K.J.; Anila E.I. Fabrication of p-SnO/n-SnO<sub>2</sub> Transparent p-n Junction Diode by Spray Pyrolysis and Extraction of Device's Intrinsic Parameters. *Materials Letter* (2019) 211-214
25. Pereira, M.S.; Lima1, F.A.S.; Silva, C.B.; Freire, P.T.C.; Vasconcelos, I.F. Structural, morphological and optical properties of SnO<sub>2</sub> nanoparticles obtained by a proteic sol-gel method and their application in dye-sensitized solar cells. *Journal of Sol-Gel. Science and Technology* 84 (2017) 206-213.
26. Bastami, H.; Taheri-Nassaj, E. Synthesis of nanosized (Co, Nb, Sm)-doped SnO<sub>2</sub> powders using coprecipitation method. *Journal of Alloys and Compounds* 495 (2010) 121-125.
27. Juhannaud, J.; Rossignol, J.; Stuerger, D. Rapid synthesis of tin (IV) oxide nanoparticles by microwave induced thermohydrolysis. *Journal of Solid State Chemistry* 181 (2008) 1439-1444.
28. Ariya Nachiar, R.; Muthukumar, S. Structural, photoluminescence and magnetic properties of Cu-doped SnO<sub>2</sub> nanoparticles co-doped with Co. *Optics & Laser Technology* 112 (2019) 458- 466.
29. SivaJahnavi, V.; Tripathy, S.K.; Ramalingeswara Rao, A V N. Structural, optical, magnetic and dielectric studies of SnO<sub>2</sub> nanoparticles in real time applications. *Physica B: Condensed Matter* 565 (2019) 61-72
30. Velásquez, C.; Rojas, F.; Ojeda, M.L.; Ortiz, A.; Campero, A. Structure and texture of self-assembled nanoporous SnO<sub>2</sub>. *Nanotechnology* 16 (2005) 1278.
31. Amalric-Popescu, D.; Bozon-Verduraz, F. Infrared studies on SnO<sub>2</sub> and Pd/SnO<sub>2</sub>. *Today* 70 (2001) 139-151.
32. Entradas, T.; Cabrita, J.F.; Dalui, S.; Nunes, M.R.; Monteiro, O.C.; Silvestre, A. Synthesis of sub-5 nm Co-doped SnO<sub>2</sub> nanoparticles and their structural, microstructural, optical and photocatalytic properties. *Materials Chemistry and Physics* 147 (2014) 563-571.
33. Roguai, S.; Djelloul, A.; Nouveau, C.; Souier, T.; Dakhel, AA.; Bououdina, M. Structure, microstructure and determination of optical constants from transmittance data of co-doped Zn<sub>0.90</sub>Co<sub>0.05</sub>M<sub>0.05</sub>O (M = Al, Cu, Cd, Na) films. *Journal of Alloys Compounds* 599 (2014) 150-158.
34. Melsheimer, J.; Ziegler, D. Band gap energy and Urbach tail studies of amorphous, partially crystalline and polycrystalline tin dioxide. *Thin Solid Films* 129 (1985) 35- 47.

35. Ajilia, M.; Castagn b, M.; Kamoun Turki, N. Spray solution flow rate effect on growth, optoelectronic characteristics and photoluminescence of SnO<sub>2</sub>:F thin films for photovoltaic application. *Optik* 126 (2015) 708-714.
36. Bansal, S.; Pandya, D.K.; Kashyap, S.C.; Haranath, D. Growth ambient dependence of defects, structural disorder and photoluminescence in SnO<sub>2</sub> films deposited by reactive magnetron sputtering. *Journal of Alloys and Compounds* 583 (2014) 186-190.

**Please cite this Article as:**

Roguai S., Djelloul A., Structural and optical analysis of SnO<sub>2</sub> thin films by spray pyrolysis, ***Algerian J. Env. Sc. Technology*, 8:1 (2022) 2285-2290**